DETECTION OF PARATRIOZA IN POTATO USING DRONE IMAGERY AND DEEP LEARNING

DETECCIÓN DE PARATRIOZA EN PAPA USANDO IMÁGENES TOMADAS POR DRONES Y APRENDIZAJE PROFUNDO

Elizabeth Martínez-Trejo[1, 2], Héctor Flores-Magdaleno[3], Remigio A. Guzmán-Plazola[4], Gabriel Otero-Colina[1], Lauro Soto-Rojas[1] and Alejandro Pérez-Panduro[1]**

[1]Colegio de Postgraduados (CP), Campus Montecillo, Posgrado Fitosanidad-Entomología y Acarología, Montecillo, Estado de México, México. [2]Universidad Mexiquense del Bicentenario, UES San José del Rincón, San José del Rincón, Estado de México, México. [3]CP, Campus Montecillo, Posgrado Hidrociencias, Montecillo, Estado de México, México. [4]CP, Campus Montecillo, Posgrado Fitosanidad-Fitopatología, Montecillo, Estado de México, México.

**Autor de correspondencia* (aperez@colpos.mx)

SUMMARY

Remote sensing from drones facilitates the detection of pests and diseases in crops. For instance, true color (RGB) and multispectral (ME) images can be used to generate vegetation indices that indicate particular plant health conditions. This study aimed to evaluate the potential of RGB and ME images, captured by drones at a height of 20 m, to detect the presence of *Bactericera cockerelli* in a potato (*Solanum tuberosum*) cv. Fianna plot. One day before the images were captured, a visual survey was conducted in the plot to locate and mark 50 potato stems whose leaves had *B. cockerelli* nymphs or eggs, and 50 stems with pest-free leaves. Orthomosaics were generated using the Pix4D software and rectified in QGIS. From these orthomosaics, three vegetation indices derived from the RGB sensor (ExG, GLI, and VIgreen) and two from the ME sensor (NDVI and NDRE) were calculated. Subsequently, the marked plants were identified in the orthomosaics, and four categories of pixels were extracted: plants with *B. cockerelli*, plants without *B. cockerelli*, soil, and shade. The images were processed using Python and the Keras library within a Multilayer Perceptron (MLP) neural network. The model performance was evaluated using the Matthews correlation coefficient (MCC), obtaining a value of 0.60 for the ME sensor bands and the NDVI and NDRE indices. This result indicates a moderate discrimination capacity, adequate to support the detection and monitoring of *B. cockerelli* in the field, although it suggests the need for further improvements to optimize early detection and timely control.

Index words: *Bactericera cockerelli*, *Solanum tuberosum*, deep learning, drone, remote sensing,

RESUMEN

La teledetección mediante sensores remotos montados en drones facilita la detección de plagas y enfermedades en cultivos; por ejemplo, las imágenes en color verdadero (RGB) y multiespectrales (ME) pueden emplearse para generar índices de vegetación que indican estados particulares de la salud de las plantas. Este estudio tuvo como objetivo evaluar el potencial de las imágenes RGB y ME, capturadas por drones a una altura de 20 m, para detectar la presencia de *Bactericera cockerelli* en un cultivo de papa (*Solanum tuberosum*) variedad Fianna. El día previo a la captura de las imágenes se realizó un muestreo visual en el cultivo para localizar y marcar 50 tallos, cuyas hojas presentaban ninfas o huevos de *B. cockerelli* y 50 tallos con hojas libres de la plaga. Se generaron ortomosaicos utilizando el software Pix4D y se rectificaron en QGIS. A partir de estos ortomosaicos, se calcularon tres índices de vegetación derivados del sensor RGB (ExG, GLI y VIgreen) y dos del sensor ME (NDVI y NDRE). Posteriormente, las plantas marcadas fueron identificadas en los ortomosaicos y se extrajeron cuatro categorías de píxeles: plantas con *B. cockerelli*, plantas sin *B. cockerelli*, suelo y sombra. Las imágenes fueron procesadas utilizando Python y la librería Keras dentro de una red neuronal de Perceptrón Multicapa (MLP). El desempeño del modelo se evaluó mediante el coeficiente de correlación de Matthews (MCC), obteniendo un valor de 0.60 para las bandas del sensor ME y los índices NDVI y NDRE. Este resultado evidencia una capacidad de discriminación moderada, adecuada para apoyar la detección y el monitoreo de *B. cockerelli* en campo, aunque sugiere la necesidad de mejoras adicionales para optimizar la detección temprana y el control oportuno.

Palabras clave: *Bactericera cockerelli*, *Solanum tuberosum*, aprendizaje profundo, dron, teledetección.

INTRODUCTION

The potato psyllid, *Bactericera cockerelli* (Šulc, 1909) (Homoptera: Triozidae), also known as paratrioza, is the most significant pest in the potato (*Solanum tuberosum* L.) crop. This insect was first reported by K. Šulc in 1909, attacking *Capsicum* sp. in Colorado, United States of America (Butler and Trumble, 2012). *Bactericera cockerelli* is responsible for transmitting the bacterium *Candidatus* Liberibacter solanacearum (CaLso), which causes potato zebra chip disease (Hansen *et al*., 2008). Furthermore, it induces potato yellowing (PY), attributed to a toxin injected into the plant during feeding (Wenninger and Rashed, 2023).

Currently, *B. cockerelli* is distributed across North and Central America, New Zealand, Australia, and some countries in Northern Europe (EPPO, 2025); however, CaLso has only been reported in the Americas and Oceania (Wenninger and Rashed, 2023).

Early CaLso infection impacts crop yield by reducing the photosynthetic rate (Gao *et al*., 2016). It also decreases starch content in tubers while increasing their reducing

Received: July 05, 2025
Accepted: April 21, 2026

DOI: https://doi.org/10.35196/rfm.2026.2.22

sugars, which negatively affects their internal appearance and taste (Wallis *et al*., 2012). Once inoculated into the leaves, CaLso reaches the tuber in just four days, whereas symptoms of CaLso in the plant become visible, both in foliage and tubers, between the third and fifth week after infection (Vereijssen *et al*., 2018). Given this short time period between inoculation and disease symptom appearance, controlling *B. cockerelli* populations is crucial throughout the entire crop cycle (Rashed *et al*., 2018; Sarkar *et al*., 2023).

The global management of this pathosystem in commercial agriculture is currently based on insecticide applications; for instance, up to 16 applications per growing cycle have been documented in the US, involving up to 11 different biochemical modes of action (Vereijssen *et al*., 2018), and incurring costs as high as $1,235 USD ha^{-1} (Eigenbrode and Gomulkiewicz, 2022).

Drone image analysis has proven to be an effective tool for detecting and monitoring insect pests in crops (Moses-Gonzales and Brewer, 2021; Subramanian *et al*., 2021). This capability enables more efficient pest control through localized applications, consequently reducing the toxicological load on crops and associated costs. This study focuses on detecting *B. cockerelli* in potato crops by analyzing RGB and multispectral (ME) images acquired by drones under field conditions. The methodological approach involves the extraction of visible-spectrum vegetation indices from RGB imagery, including the Excess Green Index (ExG), Green Leaf Index (GLI) and Green Vegetation Index (VIgreen), as well as the calculation of multispectral indices such as the Normalized Difference Vegetation Index (NDVI) and the Normalized Difference Red Edge Index (NDRE). These spectral features are used as inputs to a multilayer perceptron model to discriminate between potato plants with and without the presence of *B. cockerelli*, thereby addressing an identified gap in the existing literature for this specific crop.

MATERIALS AND METHODS

Study site

The study was conducted in a commercial potato field located in the municipality of Villa Victoria, State of Mexico, Mexico (coordinates 19° 30′ 3.85″ N, 100° 06′ 50.15″ W) during the 2024 growing season. Planting was carried out on July 20th (tuber bulking stage) using the Fianna cultivar, a white-tuber potato with an intermediate growth cycle (120 days). The study area had a high prevalence of *B. cockerelli*.

Visual sampling of *Bactericera cockerelli* in the field

A visual monitoring of *B. cockerelli* was conducted on the leaves of individual potato plant stems (sampling unit). The day before the flights, where images for this study were captured, all leaves of individual potato stems were examined to locate (and mark) 50 stems with the presence of nymphs or eggs, as well as 50 stems free from infestation. Infested stems were marked with a red flag, while uninfested stems were marked with a yellow flag. These flags unequivocally identified the marked stems in the resulting orthomosaics. We avoided stems with leaves showing typical symptoms of *Alternaria solani*, *Phytophthora infestans*, or any other symptom that could introduce noise to the model.

Image acquisition

RGB and ME images were captured during separate flights conducted on October 19th, 91 days after sowing (maturity and harvesting). RGB images were taken with a DJI Phantom 4 Pro® drone (DJI, Shenzhen, Guangdong, China), equipped with a 1-inch, 20-megapixel CMOS sensor. ME images were captured using a Parrot Sequoia Plus® camera (3D Robotics, Berkeley, California, USA), adapted to a DJI Matrice 300 RTK drone (DJI Ltd., Shenzhen, China). Both flights were performed at a height of 20 m. The ME camera features four sensors: green (550 ± 40 nm), red (660 ± 40 nm), red edge (735 ± 10 nm) and near-infrared (NIR) (790 ± 40 nm), with a single-band resolution of 1.2 MP (1280 × 960 px). Additionally, it incorporates a sunshine sensor to compensate for changes in light during flight, alongside automatic radiometric calibration. This process corrects for variations in ambient illumination and sensor response, converting raw digital numbers into surface reflectance values, which is essential to ensure consistency and comparability of spectral measurements across different flights and acquisition conditions.

Images from both sensors were acquired under clear sky conditions with 75 % side overlap and 85 % front overlap for both flights. The captured images were processed using Pix4D software (Pix4D SA, Lausanne, Switzerland); for ME images, the software corrected the estimated reflectance and performed radiometric calibration (sharpness) via a calibration panel. The resulting pixel size was 0.5 cm/pixel for the RGB orthomosaic and 3 cm/pixel for the ME orthomosaic. The latter was selected to reduce the computational resource demand during model training; resampling was performed in QGIS by defining the grid extent and cell size within the Raster Calculator.

Orthomosaic rectification was performed using the QGIS Version 3.34.8-Prizren Georeferencer tool. This process utilized easily identifiable ground control points (GCPs),

including plant marking flags and checkered square plates, which were present in the original images. A first-degree polynomial transformation was applied employing the nearest neighbor resampling method. The resulting RGB orthomosaic demonstrated strong agreement with the corresponding ME images, exhibiting a root mean square error (RMSE) of 0.16 pixels.

Data processing

Several vegetation indices were computed from the orthomosaic bands using the Raster Calculator in QGIS (v. 3.34.8-Prizren). The Excess Green Index (ExG), Green Leaf Index (GLI) and Green Vegetation Index (VIgreen) were derived from the RGB imagery. Additionally, the Normalized Difference Vegetation Index (NDVI) and the Normalized Difference Red Edge Index (NDRE) were calculated from the multispectral (ME) data (Table 1).

Band and index values were extracted in QGIS by manually delineating a polygon shapefile layer over the RGB orthomosaic. Each polygon was assigned to one of four target categories: soil, shade, plants infested with *B. cockerelli*, and healthy plants. The training dataset was generated by extracting pixel values within these polygons and aggregating them at the plant level prior to data partitioning (Figure 1).

Prediction map and detection of *Bactericera cockerelli*

The prediction map was generated through the development and training of a Multilayer Perceptron (MLP) artificial neural network**.** This network was configured with four target classes: a) plants with *B. cockerelli* (nymphs or nymphs and eggs), b) plants without *B. cockerelli*, c) soil, and d) shade. The predictor variables included ME and RGB sensor bands, both individually and combined with their respective derived indices (Table 1).

The prediction map generated from the MLP was constructed with five densely connected layers. This network included an input layer with 256 units and three hidden layers containing 128, 54 and 8 units, respectively. The output layer consisted of four neurons, corresponding to the four classes, with a softmax activation function (Goodfellow *et al*., 2016). Adam (Adaptive Moment Estimation) (Kingma and Ba, 2015) served as the optimization algorithm.

The MLP was trained for a maximum of 200 epochs with a batch size of 32. To mitigate overfitting, L2 kernel regularization was integrated into the architecture, and an EarlyStopping callback was implemented to monitor validation loss. Training was automatically halted if no improvement in validation loss occurred within a predefined period (patience values of 5, 10 and 20 were evaluated), after which the best-performing weights were restored. Furthermore, various L2 regularization coefficients (0.0001, 0.001 and 0.01) were assessed to determine the optimal configuration. A dedicated validation set was used throughout the process to guide model selection and ensure convergence control.

The model was implemented in Python using the Keras (TensorFlow) library (Chollet, 2017) and Google Colab. To prevent data leakage, 30 % of the digitized polygons were reserved for model testing; this ensured that all pixels from a specific polygon were assigned exclusively to a single subset of data, preventing spatial correlation between training and testing data. All hidden layers in the MLP utilized the Rectified Linear Unit (ReLU) activation function.

Metrics

The metrics used to evaluate the model were derived from the confusion matrix, which indicates the proportion of correct or incorrect classifications for each class.

Table 1. Vegetation indices derived from RGB and multispectral sensors used as predictors for the presence of *Bactericera cockerelli* in potato plants.

Index	Name	Formula	Reference
ExG	Excess green	*2g-r-b*	Woebbecke *et al*. (1995)
GLI	Green leaf index	*(2G-R-B)/(2G+R+B)*	Louhaichi *et al*. (2001)
VIgreen	Green vegetation index	*(G-R)/(G+R)*	Gitelson *et al*. (2002)
NDVI	Normalized difference Vegetation index	*(NIR-RED)/(NIR+RED)*	Rouse (1973)
NDRE	Normalized difference Red edge	*(NIR-RD)/(NIR+RD)*	Barnes *et al*. (2000)

NIR: near-infrared, RD: red edge, RED: red.

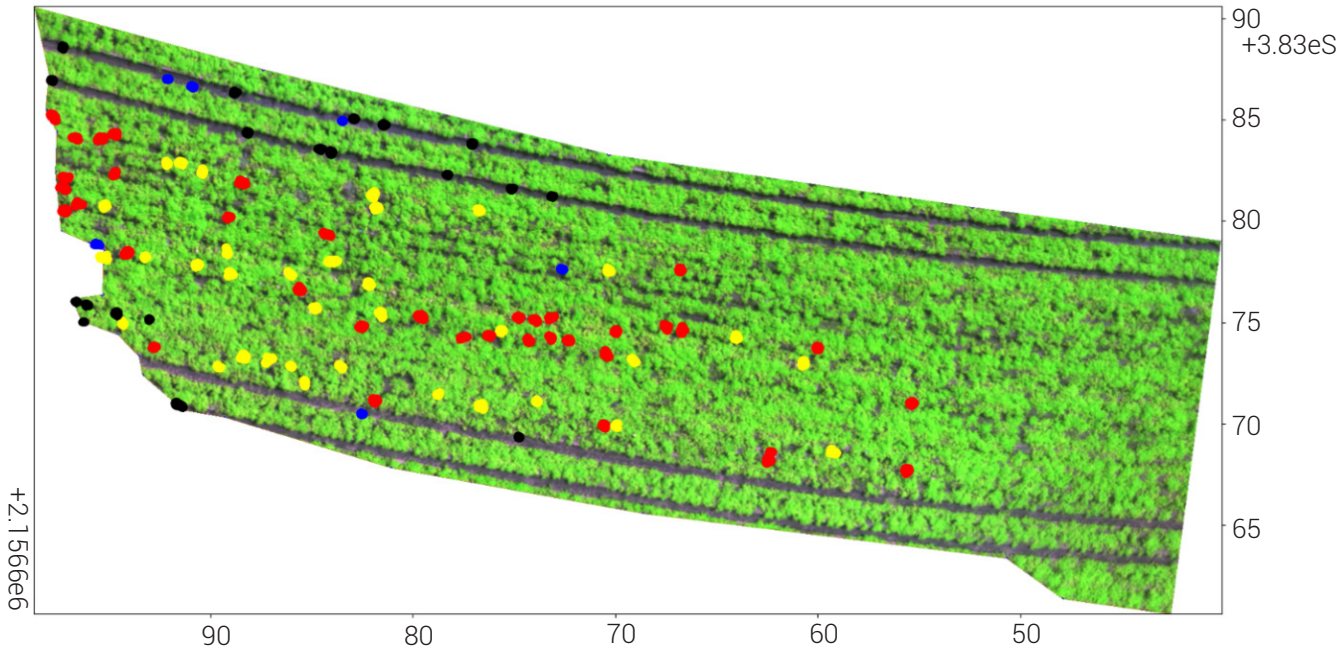

Figure 1. Training data based on visual field inspection one day before the flight. Red: plants with *Bactericera cockerelli*, yellow: plants without *B. cockerelli*, black: shade and blue: soil.

Additionally, Matthews correlation coefficient (MCC) was used for imbalanced classes (Tharwat, 2018) (Table 2).

Permutation importance

The importance of predictor variables on estimation accuracy was determined using the Permutation Importance method within scikit-learn. This method randomly shuffles the values of each variable, one at a time, and assesses the resulting change in estimation accuracy. If shuffling a variable lead to a decrease in accuracy, it indicates that the variable is important (Breiman, 2001). This calculation was performed using the scikit-learn machine learning library (Pedregosa *et al*., 2011).

RESULTS

Visual detection of *Bactericera cockerelli* in the field

In the sample of 50 stems infested, there was an average of 5.16 nymphs per stem, with a range from one to 18; more than 50 % of stems had only one to three nymphs.

Multilayer perceptron training

The combination of ME bands with the NDVI and NDRE indices yielded the highest Matthews correlation coefficient (MCC) at 0.60 and accuracy of 0.73. With this same combination of predictor variables, the 'without *B. cockerelli*' class was classified with a precision of 0.64, a recall of 0.69, and an F1-score of 0.67. For the 'with *B. cockerelli*' class, all metrics (precision, recall, and F1-score) were 0.68, 0.63 and 0.65, respectively (Table 3).

The combination that produced the second-best metrics involved the ME sensor. Its MCC was 0.59. For the 'without *B. cockerelli*' class, precision was 0.62, recall was 0.70 and F1-score was 0.66. For the 'with *B. cockerelli*' class, these metrics were 0.67, 0.58 and 0.63, respectively (Table 3).

Hierarchy of predictors for the studied classes

Among the predictor variables derived from the ME sensor + indices (Red, NIR, Red Edge, Green, NDVI and NDRE), the NIR (0.3498 ± 0.0050) and Red (0.1325 ± 0.0047) bands showed greater relative importance than the others for all classes ('with *B. cockerelli*', 'without *B. cockerelli*', soil, and shade). For the variables derived from the ME sensor, spectral bands (Red, Green, Red Edge and NIR), Red (0.2648 ± 0.0044) and NIR (0.1512 ± 0.0046) were the most relevant.

Prediction map

Using the combination of variables that yielded the best results (ME + NDVI and NDRE), a prediction map was created, encompassing the four analyzed categories (Figure 2). On this map, pixels indicating *B. cockerelli* infestation are shown in yellow, uninfested pixels in green, shade in black, and soil in brown. This prediction achieved an MCC of 0.60.

Table 2. Metrics used to evaluate the multilayer perceptron model and their corresponding formulas.

Name	Formula
Accuracy	$(TP + TN) / (TP + FP + FN + TN)$
Recall	$TP / (TP + FN)$
Precision	$TP / (TP + FP)$
F1-score	$2TP / (FP + 2TP + FN)$
MCC	$[(TP \times TN) - (FP \times FN)] / \sqrt{([(TP+FP)(TP+FN)(TN+FP)(TN+FN)])}$

TP, TN, FN and FP are true positives, true negatives, false negatives and false positives, respectively. MCC: Matthews correlation coefficient.

Table 3. Metrics obtained from processing presence and absence data of *Bactericera cockerelli* nymphs in potato using the Multilayer Perceptron model.

Predictor variables	Metrics	Class			
		Without *B. cockerelli*	With *B. cockerelli*	Soil	Shade
RGB	Precision	0.59	0.57	0.95	0.94
	Recall	0.46	0.68	0.90	1.00
	F1-score	0.51	0.62	0.92	0.97
	Accuracy	0.67			
	MCC	0.51			
RGB+ExG+GLI+VIgreen	Precision	0.60	0.61	0.97	0.99
	Recall	0.59	0.62	0.98	1.00
	F1-score	0.60	0.61	0.97	0.99
	Accuracy	0.70			
	MCC	0.55			
ME	Precision	0.62	0.67	0.95	0.97
	Recall	0.70	0.58	0.95	0.98
	F1-score	0.66	0.63	0.95	0.98
	Accuracy	0.72			
	MCC	0.59			
ME + NDVI + NDRE	Precision	0.64	0.68	0.96	0.97
	Recall	0.69	0.63	0.93	0.99
	F1-score	0.67	0.65	0.94	0.98
	Accuracy	0.73			
	MCC	0.60			

RGB: red, green and blue, ExG: excess green, GLI: green leaf index, VIgreen: green vegetation index, ME: multispectral bands including red, near-infrared, red edge and green, NDVI: normalized difference vegetation index, NDRE: normalized difference red edge, MCC: Matthews correlation coefficient.

DISCUSSION

To the best of our knowledge, this is the first report of an effort to detect *B. cockerelli* using remote sensors (drone-captured images). Previous studies of this type (analysis of drone-captured field images and machine learning tools) in potatoes have focused on detecting either diseases (León-Rueda *et al*., 2022; Rodríguez *et al*., 2021) or physiological disorders (León-Rueda *et al*., 2022). Another research analyzed tuber slice laboratory images to evaluate zebra chip severity using neural networks (Hernández-Deheza *et al*., 2020).

In this study, an MLP artificial neural network was employed to detect *B. cockerelli* in potato plants by integrating RGB and multispectral (ME) sensor data along with their vegetation-derived indices. Prior research has reported that MLP models achieve competitive performance in classification tasks compared to algorithms such as Random Forest or Support Vector Machines (Benos *et al*., 2021). This is largely because the relationship between information captured by sensors and a plant physiological state is often non-linear (Ballesteros *et al*., 2020), but MLP are well-suited for identifying non-linear relationships between input and output datasets (Popescu *et al*., 2009).

The ME sensor bands demonstrated predictive capability for the presence (current or recent) of *B. cockerelli* in potato plants (MCC = 0.59) (Table 3); however, including the NDVI and NDRE vegetation indices**,** derived from its bands, substantially increased the neural network predictive capability (MCC = 0.60). This observation aligns with findings by León-Rueda *et al*. (2022) in their study on detecting diseases and physiological disorders in potatoes.

From the ME sensor**,** the NIR and Red bands provided the most information to the model for detecting *B. cockerelli* infestations, 0.34 and 0.13 respectively. It was previously known about insect-induced changes in the spectral characteristics of leaves in the infrared (Kharuf-Gutierrez *et al*., 2018; Marston *et al*., 2020; Vanegas *et al*., 2018). It is also known that a single *B. cockerelli* nymph can cause a physiological disorder (Carter, 1939) manifested by slight leaf curling and chlorosis of the leaves (Sengoda *et al*., 2010), caused by salivary secretions during stylet penetration into plant tissues (Hansen *et al*., 2008).

While *B. cockerelli* is the primary pest in the study area, plants showing symptoms of other diseases or physiological disorders were excluded during dataset curation. Consequently, a fifth category was not

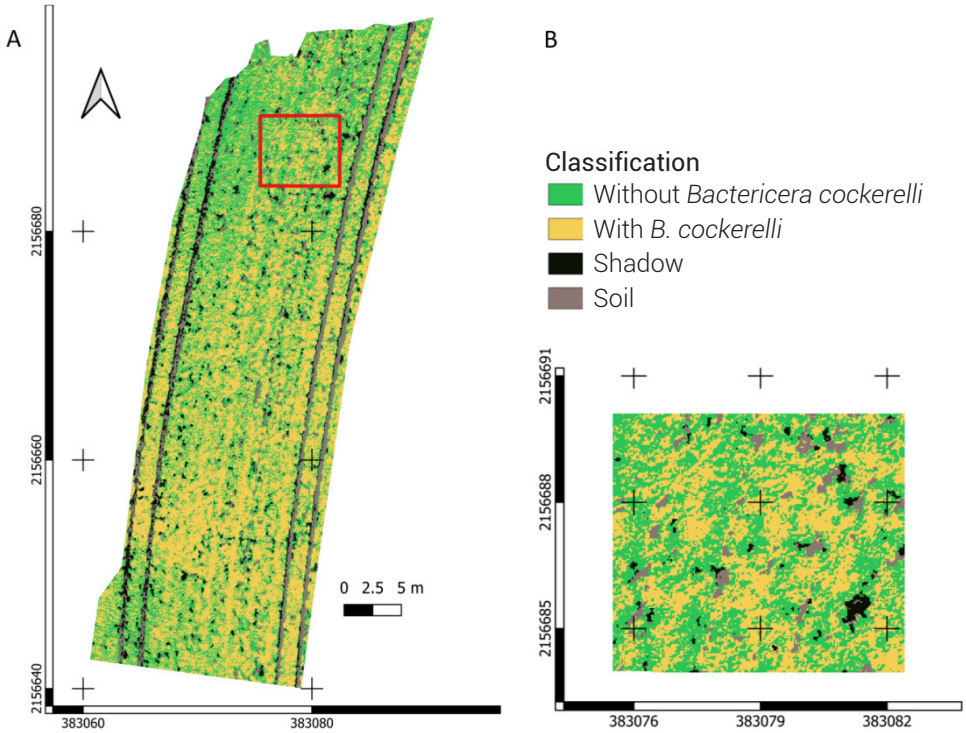

Figure 2. Prediction map of the presence/absence of *Bactericera cockerelli* in field-grown potato cv. Fianna, generated by using the Multilayer Perceptron model with multispectral bands and the NDVI and NDRE indices as predictor variables. A) full map, B) enlarged segment of the map to improve class visualization.

defined, and the model was trained only on the four pre-stablished classes. This approach may limit the model robustness under field conditions where multiple stresses simultaneously co-occur; therefore, future research should incorporate additional classes representing other biotic and abiotic factors to facilitate multi-stress discrimination.

In the study region, producers usually apply systemic and contact pesticides every 3-4 days to control *B. cockerelli*, late blight and other pathogens. This intensive management, often exceeding 30 applications per season (Rubio *et al*., 2006), underscores an urgent need to reduce the crop pesticide load. The results of this study contribute to this objective by enabling the spatial identification of infestation foci through the MLP model, marking a significant step toward site-specific pest management. Nevertheless, these findings should be treated as a proof of concept. Further validation involving larger sample sizes, diverse geographic locations, multiple growing seasons, and different potato varieties is essential before its operational deployment in integrated pest management programs.

CONCLUSIONS

This study developed an MLP-based classification model to detect the presence of *Bactericera cockerelli* nymphs on potato plants, achieving an MCC of 0.60 for identifying pixels with current or recent infestation. The best performance was obtained using ME sensor bands with NDVI and NDRE indices, demonstrating the potential of drone-acquired multispectral imagery for detection of damage by nymphs and site-specific pest management. This level of performance is suitable for decision support and field monitoring, although not yet for fully autonomous deployment. Nevertheless, as the study was conducted on a single cultivar, location and growing season, further validation across diverse environments, growing seasons, and cultivars is necessary prior to operational implementation.

ACKNOWLEDGMENTS

The authors gratefully acknowledge the support of Secretaría de Ciencias, Humanidades, Tecnología e Innovación for the scholarship awarded to the first author, which made this study possible.

BIBLIOGRAPHY

Ballesteros R., D. S. Intrigliolo, J. F. Ortega, J. M. Ramírez-Cuesta, L. Buesa and M. A. Moreno (2020) Vineyard yield estimation by combining remote sensing, computer vision and artificial neural network techniques. *Precision Agriculture* 21:1242-1262, https://doi.org/10.1007/s11119-020-09717-3

Barnes E., R. Clarke, S. E. Richards, P. D. Colaizzi, J. Haberland, M. Kostrzewski, … and M. S. Moran (2000) Coincident detection of crop water stress, nitrogen status, and canopy density using ground based multispectral data. *In*: Proceedings of the Fifth International Conference on Precision Agriculture. ASA-CSSA-SSSA. Madison, Wisconsin, USA. pp:1-15.

Benos L., A. C. Tagarakis, G. Dolias, R. Berruto, D. Kateris and D. Bochtis (2021) Machine learning in agriculture: a comprehensive updated review. *Sensors* 21:3758, https://doi.org/10.3390/s21113758

Breiman L. (2001) Random forests. *Machine Learning* 45:5-32, https://doi.org/10.1023/a:1010933404324

Butler C. D. and J. T. Trumble (2012) The potato psyllid, *Bactericera cockerelli* (Sulc) (Hemiptera: Triozidae): life history, relationship to plant diseases, and management strategies. *Terrestrial Arthropod Reviews* 5:87-111, https://doi.org/10.1163/187498312X634266

Carter W. (1939) Injures to plants caused by insect toxins. *The Botanical Review* 5:273-326, https://doi.org/10.1007/BF02878504

Chollet F. (2017) Deep Learning with Python. Manning Publications Company. Shelter Island, New York, USA. 384 p.

Eigenbrode S. D. and R. Gomulkiewicz (2022) Manipulation of vector host preference by pathogens: implications for virus spread and disease management. *Journal of Economic Entomology* 115:387-400, https://doi.org/10.1093/jee/toab261

EPPO, European and Mediterranean Plant Protection Organization (2025) EPPO Global Database. *Bactericera cockerelli*. European and Mediterranean Plant Protection Organization. Paris, France. https://gd.eppo.int/taxon/PARZCO/distribution (June 2025).

Gao F., Z. H. Zhao, J. Jifon and T. X. Liu (2016) Impact of potato psyllid density and timing of infestation on Zebra chip disease expression in potato plants. *Plant Protection Science* 52:262-269, https://doi.org/10.17221/186/2015-PPS

Gitelson A. A., Y. J. Kaufman, R. Stark and D. Rundquist (2002) Novel algorithms for remote estimation of vegetation fraction. *Remote Sensing of Environment* 80:76-87, https://doi.org/10.1016/S0034-4257(01)00289-9

Goodfellow I., Y. Bengio and A. Courville (2016) Deep feedforward networks. *In*: Deep Learning. I. Goodfellow, Y. Bengio and A. Courville (eds.). MIT Press. Cambridge, Massachusetts, USA. pp:164-223.

Hansen A. K., J. T. Trumble, R. Stouthamer and T. D. Paine (2008) A new huanglongbing species, "*Candidatus* Liberibacter psyllaurous" found to infect tomato and potato, is vectored by the psyllid *Bactericera cockerelli* (Sulc). *Applied and Environmental Microbiology* 74:5862-5865, https://doi.org/10.1128/AEM.01268-08

Hernández-Deheza M. G., R. I. Rojas-Martínez, A. Rivera-Peña, E. Zavaleta-Mejía, D. L. Ochoa-Martínez and J. A. Carrillo-Salazar (2020) Evaluation of zebra chip using image analysis. *American Journal of Potato Research* 97:586-595, https://doi.org/10.1007/s12230-020-09807-y

Kharuf-Gutiérrez S., L. Hernández-Santana, R. Orozco-Morales, O. C. Aday D. e I. Delgado M. (2018) Análisis de imágenes multiespectrales adquiridas con vehículos aéreos no tripulados. *Revista de Ingeniería Electrónica, Automática y Comunicaciones* 39:79-91.

Kingma D. P. and J. Ba (2015) Adam: a method for stochastic optimization. 3rd International Conference for Learning Representations, San Diego, 2015. *arXiv*:1412.6980v9, https://doi.org/10.48550/arXiv.1412.6980

León-Rueda W. A., C. León, S. Gómez-Caro and J. G. Ramírez-Gil (2022) Identification of diseases and physiological disorders in potato via multispectral drone imagery using machine learning tools. *Tropical Plant Pathology* 47:152-167, https://doi.org/10.1007/s40858-021-00460-2

Louhaichi M., M. M. Borman and D. E. Johnson (2001) Spatially located platform and aerial photography for documentation of grazing impacts on wheat. *Geocarto International* 16:65-70, https://doi.org/10.1080/10106040108542184

Marston Z. P. D., T. M. Cira, E. W. Hodgson, J. F. Knight, I. V. Macrae and R. L. Koch (2020) Detection of stress induced by soybean aphid (Hemiptera: Aphididae) using multispectral imagery from unmanned aerial vehicles. *Journal of Economic Entomology* 113: 779-786, https://doi.org/10.1093/jee/toz306

Moses-Gonzales N. and M. J. Brewer (2021) A special collection: drones to improve insect pest management. *Journal of Economic Entomology* 114:1853-1856, https://doi.org/10.1093/jee/toab081

Pedregosa F., G. Varoquaux, A. Gramfort, V. Michel, B. Thirion, O. Grisel, … and E. Duchesnay (2011) Scikit-learn: machine learning in Python. *Journal of Machine Learning Research* 12:2825-2830.

Popescu M. C., V. E. Balas, L. Perescu-Popescu and N. Mastorakis (2009) Multilayer perceptron and neural networks. *WSEAS Transactions on Circuits and Systems* 8:579-588.

Rashed A., N. Olsen, C. M. Wallis, L. Paetzold, L. Woodell, M. Rashidi, … and C. M. Rush (2018) Postharvest development of '*Candidatus* Liberibacter solanacearum' in late-season infected potato tubers under commercial storage conditions. *Plant Disease* 102:561-568, https://doi.org/10.1094/pdis-05-17-0619-RE

Rodríguez J., I. Lizarazo, F. Prieto and V. Angulo-Morales (2021) Assessment of potato late blight from UAV-based multispectral imagery. *Computers and Electronics in Agriculture* 184:106061, https://doi.org/10.1016/j.compag.2021.106061

Rouse J. W. (1973) Monitoring the vernal advancement and retrogradation (green wave effect) of natural vegetation. Progress Report No. 7. Remote Sensing Center, Texas A & M University. College Station, Texas, USA. 8 p. https://ntrs.nasa.gov/citations/19740022555 (May 2025).

Rubio C. O. A., I. H. Almeyda L., J. Ireta M., J. A. Sánchez S., R. Fernández S., J. T. Borbón S., … y M. A. Cadena H. (2006) Distribución de la punta morada y *Bactericera cockerelli* Sulc. en las principales zonas productoras de papa en México. *Agricultura Técnica en México* 32:201-211.

Sarkar S. C., S. Hatt, A. Philips, M. Akter, S. P. Milroy and W. Xu (2023) Tomato potato psyllid *Bactericera cockerelli* (Hemiptera: Triozidae) in Australia: incursion, potential impact and opportunities for biological control. *Insects* 14:263, https://doi.org/10.3390/insects14030263

Sengoda V. G., J. E. Munyaneza, J. M. Crosslin, J. L. Buchman and H. R. Pappu (2010) Phenotypic and etiological differences between psyllid yellows and zebra chip diseases of potato. *American Journal of Potato Research* 87:41-49, https://doi.org/10.1007/s12230-009-9115-x

Subramanian K. S., S. Pazhanivelan, G. Srinivasan, R. Santhi and N. Sathiah (2021) Drones in insect pest management. *Frontiers in Agronomy* 3:640885, https://doi.org/10.3389/fagro.2021.640885

Šulc K (1909) *Trioza cockerelli* n.sp., a novelty from North America, being also of economic importance. *Acta Societatis Entomologicae Bohemiae* 6:102-108.

Tharwat A. (2018) Classification assessment methods. *Applied Computing and Informatics* 17:168-192, https://doi.org/10.1016/j.aci.2018.08.003

Vanegas F., D. Bratanov, K. Powell, J. Weiss and F. Gonzalez (2018) A novel methodology for improving plant pest surveillance in vineyards and crops using UAV-based hyperspectral and spatial data. *Sensors* 18:260, https://doi.org/10.3390/s18010260

Vereijssen J., G. R. Smith and P. G. Weintraub (2018) *Bactericera cockerelli* (Hemiptera: Triozidae) and *Candidatus* Liberibacter solanacearum in potatoes in New Zealand: biology, transmission, and implications for management. *Journal of Integrated Pest Management* 9:13, https://doi.org/10.1093/jipm/pmy007

Wallis C., A. Rashed and C. M. Rush (2012) Large-scale shifts in potato (*Solanum tuberosum*) tuber physiology occur following infection by '*Candidatus* Liberibacter solanacearum'. *Phytopathology* 102:129-130.

Wenninger E. J. and A. Rashed (2023) Biology, ecology and management of the potato psyllid, *Bactericera cockerelli* (Hemiptera: Triozidae), and zebra chip disease in potato. *Annual Review of Entomology* 69:139-157, https://doi.org/10.1146/annurev-ento-020123-014734

Woebbecke D. M., G. E. Meyer, K. Von Bargen and D. A. Mortensen (1995) Color indices for weed identification under various soil, residue, and lighting conditions. *Transactions of the American Society of Agricultural and Biological Engineers* 38:259-269, https://doi.org/10.13031/2013.27838